Geo-Marine Letters (2024) 44:13
https://doi.org/10.1007/s00367-024-00775-4

RESEARCH

Morphotectonic characteristics of the Andaman volcanic arc and its adjoining regions, Andaman Sea

K. K. Aswini[1] · K. A. Kamesh Raju[1,2] · C. M. Bijesh[2] · V. Yatheesh[1] · N. F. K. Zeba[1] · Pawan Dewangan[1]

Received: 31 August 2023 / Accepted: 6 July 2024

Abstract

The oblique subduction of the Indian Plate beneath the Sunda Plate has resulted in the formation of diverse morphotectonic structures and major changes to the seafloor topography in the Andaman Sea, northeastern Indian Ocean. Inner volcanic arc, sliver fault system, narrow oceanic basins and backarc basins are the principal morphotectonic elements that influenced the tectonic setting and geodynamics of the Andaman backarc region. The volcanoes and fault systems in Myanmar and Sumatra are well studied, but we know relatively less about the morphotectonics of the submarine volcanoes and sliver fault networks in the Andaman Sea, that connect the volcanoes and fault systems in Myanmar and Sumatra. In the present study, we compiled the all-available high resolution bathymetry data which covers an area of approximately 140,000 km^2 in the Andaman backarc region and provided a detailed morphotectonic analysis of each of the tectonic elements. The data show 33 submarine volcanoes of varying dimension in the Andaman Sea, that stretches from the dormant Narcondam volcano to the north of Sumatra Island. In addition, the major fault systems such as Great Sumatra Fault, West Andaman Fault and Andaman Nicobar Fault that starts from northern Sumatra and ends with Andaman Backarc Spreading Centre delineated from the high-resolution bathymetry data are analysed. Northward extension of the Great Sumatra Fault furcates into several branches, which produce narrow oceanic basins. The existence of submarine volcanoes situated in the middle of these basins indicate that the Andaman-Nicobar-Sumatra volcanic arc traverses through this narrow basinal area. The occurrence of well-developed cratered volcanoes, frequent earthquake swarms and gas emanations through the flanks of the cratered seamount suggest that the off Nicobar region between 6ºN to 8ºN is the most active part of the volcanic arc during the recent past.

Keywords Submarine volcanic arc · Sliver fault systems · Bathymetry · Morphology · Andaman Sea

Introduction

Andaman-Nicobar-Sumatra subduction process mainly involves three major plates such as India-Australia, Burmese and Sunda Plate. Andaman Sea is referred as an extensional backarc basin located in the Andaman-Nicobar-Sumatra subduction zone in the Indian Ocean, which formed due to the extensional force associated with the subduction (Kamesh Raju et al. 2004, 2020; Curray 2005). Andaman backarc region consists of main tectonic features such as sliver fault system, volcanic arc and Andaman Backarc Spreading Centre (ABSC, Fig. 1) (Kamesh Raju et al. 2004; Curray 2005). The volcanic arc chain extending from inactive volcanoes in the Myanmar, Narcondam and Barren Island in the north to the Sumatra arc in the south (Curray 2005; Kamesh Raju et al. 2012a; Tripathi et al. 2017). The subduction of the Indo-Australian Plate beneath the Sunda plate which led to the melting of the subducted crust and melted magma rises to the surface through fissures and fractures, resulting in the formation of chain of volcanoes in the Andaman-Nicobar-Sumatra subduction zone (Curray 2005; Kamesh Raju et al. 2012a, 2020).

The trench-parallel motion occurring due to the oblique subduction between the Indo-Australian plate and Sunda plate is largely accommodated by the sliver fault system (Fitch 1972; Curray 2005; McCaffrey 2009; Singh et al. 2013; Moeremans and Singh 2015). The submarine volcanic arc and sliver fault system present in the Andaman Sea play a major role in the stress distribution and occurrence

✉ K. K. Aswini
aswinik@nio.org; aswini.kk5@gmail.com

[1] CSIR-National Institute of Oceanography, Dona Paula, Goa 403004, India

[2] National Centre for Polar and Ocean Research, Ministry of Earth Sciences, Vasco-da-Gama, Goa 403804, India

Published online: 01 August 2024

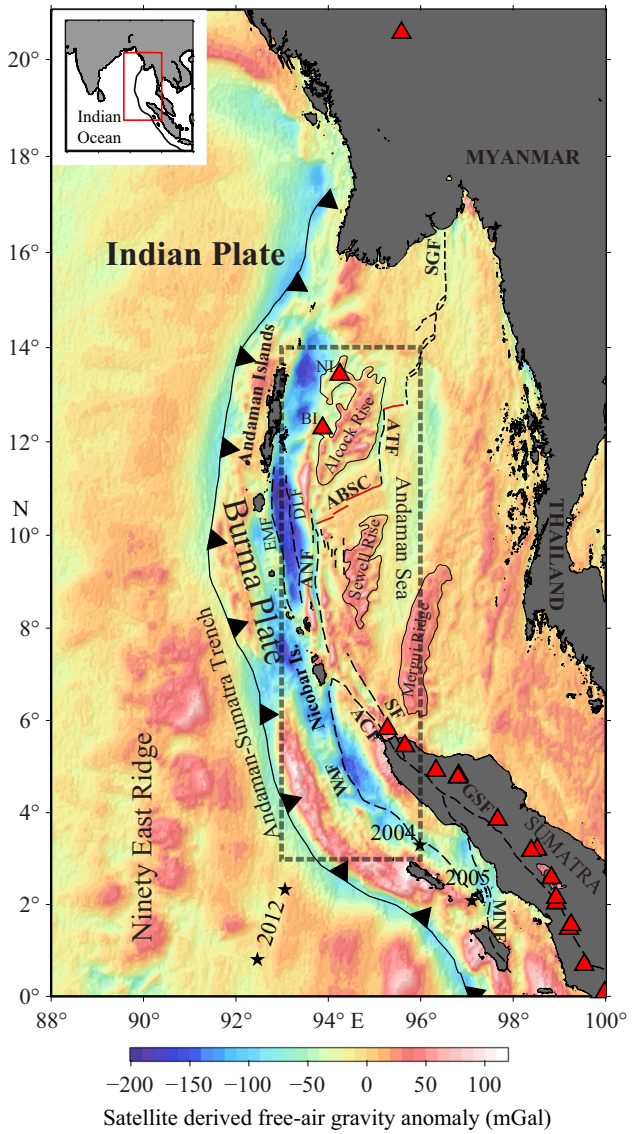

Fig. 1 Satellite derived free-air gravity anomaly map of Andaman Nicobar Subduction Zone and the adjacent areas (Sandwell et al. 2021). The dashed black lines represent the major faults (Kamesh Raju et al. 2004, 2007; Tsutsumi and Sato 2009; Cochran 2010; Singh et al. 2013). The black bordered red triangles represent the subaerial volcanoes (Sheth et al. 2009; Bandopadhyay and Carter 2017). The thick red lines indicate the Andaman Backarc Spreading Centre (Kamesh Raju et al. 2004). The black stars represent the locations of major earthquakes of 2004 and 2012. ABSC: Andaman Backarc Spreading Centre; NI: Narcondam Island; BI: Barren Island; EMF: Eastern Margin Fault; DLF: Diligent Fault; ANF: Andaman-Nicobar Fault; WAF: West Andaman Fault; ACF: Aceh Fault; SF: Seulimeum Fault; GSF: Great Sumatra Fault; MNF: Mentawai Fault; ATF: Andaman Transform Fault; SGF: Sagaing Fault. Thick black dashed rectangle represents the study area

of earthquakes in the backarc region. The sliver fault system includes the Sagaing Fault (SGF) in the Myanmar, which is connected through Andaman Transform Fault (ATF) to ABSC in the middle, and Andaman Nicobar Fault (ANF), West Andaman Fault (WAF) and the Great Sumatra Fault (GSF) in the south (Fig. 1) (Curray 2005; Diehl et al. 2013; Singh et al. 2013). In the backarc of the Andaman Sea, the boundary between the sliver fault, Burma Plate, and Sunda Plate comprises a network of arc-parallel transforms and arc-normal ridges. This boundary extends to the right-lateral Sumatra fault along the volcanic arc in the southwest. The association with the Sagaing Fault to the northeast appears less definitive, with various proposed geometries (Rangin et al. 1999; Curray 2005). As the Burma Plate is pulled northward relative to the Sunda Plate by the subducting Indian-Australian plate, "pull-apart" basins emerge along the plate boundary, leading to northeast-southwest extension of the Andaman Sea (Curray 2005; McCaffrey 2009). While "pull-apart" typically denotes intracrustal extension along a strike-slip system, the extension in the Andaman Sea involves the genesis of new crust (Kamesh Raju et al. 2004), supporting the identification of the sliver as a distinct plate. This mode of transtensional backarc opening is also known as "rhombochasm" (Rodolfo 1969; Curray 2005) or "leaky-transform" (Thompson and Melson 1972; Uyeda and Kanamori 1979; Taylor et al. 1994). SGF is mainly a continental right lateral strike slip fault extended from Myanmar to the northern Andaman Sea (Bertrand and Rangin 2003; Htet et al. 2022; Diehl et al. 2013). Southern end of this SGF connected to the ABSC with a large transform fault ATF (Singh and Moeremans 2017; Yatheesh et al. 2021). ANF is the main strike-slip fault lying north–south direction referred as a boundary between Andaman forearc and backarc basins (Cochran 2010; Singh et al. 2013). GSF is approximately 1900 km long strike-slip fault that extends from the northwestern part of Sumatra, Indonesia, to the Nicobar Islands in the Andaman Sea (Sieh and Natawidjaja 2000; Ghosal et al. 2012). GSF has indeed been recognized as an active fault since 2 Ma (Sieh and Natawidjaja 2000). WAF is situated south of the Nicobar Island considered as a back thrust fault (Kamesh Raju et al. 2007; Singh et al. 2013). In the off Nicobar region, the ANF, WAF and GSF meet at a junction where the closely spaced seamount chain is seen forming a part of the volcanic arc. This region is witnessing intense seismicity with the frequent occurrence of earthquake swarms in 2005, 2014, 2015 and 2019. Recent studies suggested that the magma movement from deeper reservoir to shallow magma chamber, triggered the reactivation of sliver fault system and cause the occurrence of earthquake swarm (Aswini et al. 2020, 2021, 2022).

Earlier research indicated that while there are active volcanoes on land in Sumatra and Java, as well as extinct and dormant volcanoes in Myanmar (Chhibber 1934; Rock et al. 1992; Zaw et al. 2017; Acocella et al. 2018; Belousov et al. 2018; Hariyono and Liliasari 2018), the Andaman Sea was considered to have a lack of active submarine volcanoes. Recent studies identified the presence of submarine

volcanoes in the Andaman Sea (Kamesh Raju et al. 2004, 2012a; Tripathi et al. 2017). Tripathi et al. 2017 identified 22 submarine volcanoes in the Andaman Sea. A combined morphotectonic analysis of the entire volcanic arc and its adjacent regions are still awaiting. In this present study, we have attempted to compile all the available high resolution bathymetry data which covered the entire inner volcanic arc of the Andaman Sea. The data allow us to identify more localized geomorphological features such as submarine volcanoes, fault systems, basins, and ridge-like features in the Andaman backarc region. Thereby we provide detailed morphotectonic analysis of these elements to improve our understanding of the dynamics of the Andaman arc volcanism.

Data and methodology

The high-resolution multibeam data acquired by CSIR-National Institute of Oceanography are used for the morphological interpretation of the study area. The presented data is the compilation all the data available with CSIR-NIO. New data are from 4 cruises, SK-89 in 1994, SSK-33 in 2012, SSK-49 in 2013 carried out onboard RV Sindhu Sankalp and SSD-046 in 2018 carried out on board RV Sindhu Sadhana are included. RV Sindhu Sankalp is equipped with Kongsberg EM302 multibeam echosounder operating at a frequency of 30 kHz. The multibeam system onboard RV Sindhu Sadhana was operated at 15 kHz frequency during the acquisition. Navigational errors resulting from the vessel movement during the survey were corrected. We collected sound velocity profiles during the survey to correct the variation of sound velocity in seawater. The multibeam data of the Andaman backarc basin were from the SK89 expedition (Kamesh Raju et al. 2004) and SSD046 expedition (Yatheesh et al. 2021), and the data from the Sumatra region were sourced from Graindorge et al. 2008. The multibeam raw data was processed using MB system. The final processed data was extracted into ASCII format and then converted into 200 m spatial resolution bathymetric grid using Generic Mapping Tool (GMT) software. This high-resolution bathymetric grid was used for the interpretation. In addition, a ~ 90 km long multi-channel seismic reflection profile (AN08Z06) in the off Nicobar region, provided by Directorate General of Hydrocarbon (DGH), India has been interpreted to understand the sub-seafloor characteristics.

Results

The multibeam bathymetry data collected in the volcanic arc region has been compiled to make a high-resolution bathymetry map of the study area (Fig. 2). The map covers an area of ~ 1,40,000 km^2 between 4°N and 14°N and depicts detailed geomorphology of the study area. The major features comprise of regional fault systems, submarine volcanic arc defined by a chain of volcanoes, and narrow basins. These are discussed in detail in the following sub-sections.

Fault systems, basins and ridge-like features

The configuration of Andaman forearc and backarc system is mainly modulated by the formation of sliver fault systems present in this region. The SGF, ATF, ABSC, ANF, WAF and GSF are the major fault and spreading center systems in the Andaman-Nicobar-Sumatra Subduction and backarc region, played a significant role in modulating the strain partitioning along the trench parallel direction. The high-resolution bathymetric map of the study region (Fig. 2) shows a notable contrast in the orientations of fault systems and the spatial layout of narrow basins. While the fault systems e.g., WAF, ANF and ATF are predominantly oriented in a near N-S trend, whereas GSF and its offshore branches exhibit a distinct SE-NW orientation. The bathymetry data revealed the fault patterns that present in the off Nicobar region, where Seulimeum Fault (SF) and Aceh Fault (ACF) of the Sumatra Fault joined with the WAF and ANF creating a triple junction approximately around 7°N (Fig. 2a). The convergence of these fault systems give rise to an intricate pattern of deformation in the surrounding area of Nicobar Island. The triple junction area is characterized by the presence of uplifted ridges at the basin's centre, making it challenging to precisely determine the connections of the strike-slip faults.

The ANF, has a generally north–south orientation to the north of Nicobar Island and is located in a narrow basin in the south that is 7 km wide around 8°N, and the rift basin deepens to approximately 4000 m and widens to about 10–20 km towards the northern portion between 8.6°N to 10°N (Fig. 2b). Its western boundary is defined by a steep marginal fault, while its eastern boundary is marked by a sedimented ridge (Fig. 2a).

A north–south trending, 50 km long, 7 km wide, elongated ridge-like feature, with its summit area reaching up to 500 m from nearby region of 2000 m water depth, is observed between ANF and the northern part of WAF at around 7°30'N (black rectangular block A in Fig. 2a). Serpentinites recovered from the eastern cliff of this block suggest mantle origin for this feature (Kamesh Raju et al. 2012b). Similar kind of two elongated ridge-like features are seen north of the above mentioned block, which is linearly configured, but not continuous (black rectangle boxes B and C in Fig. 2a).

The seismic profile (Figs. 3 & 4) passing through ~ 8°N (Fig. 3a) with NNE-SSW trend shows 7 km wide narrow basin present at the base of a 1200 m wide deep scarp. The sedimentary layers in the basin reach a maximum thickness

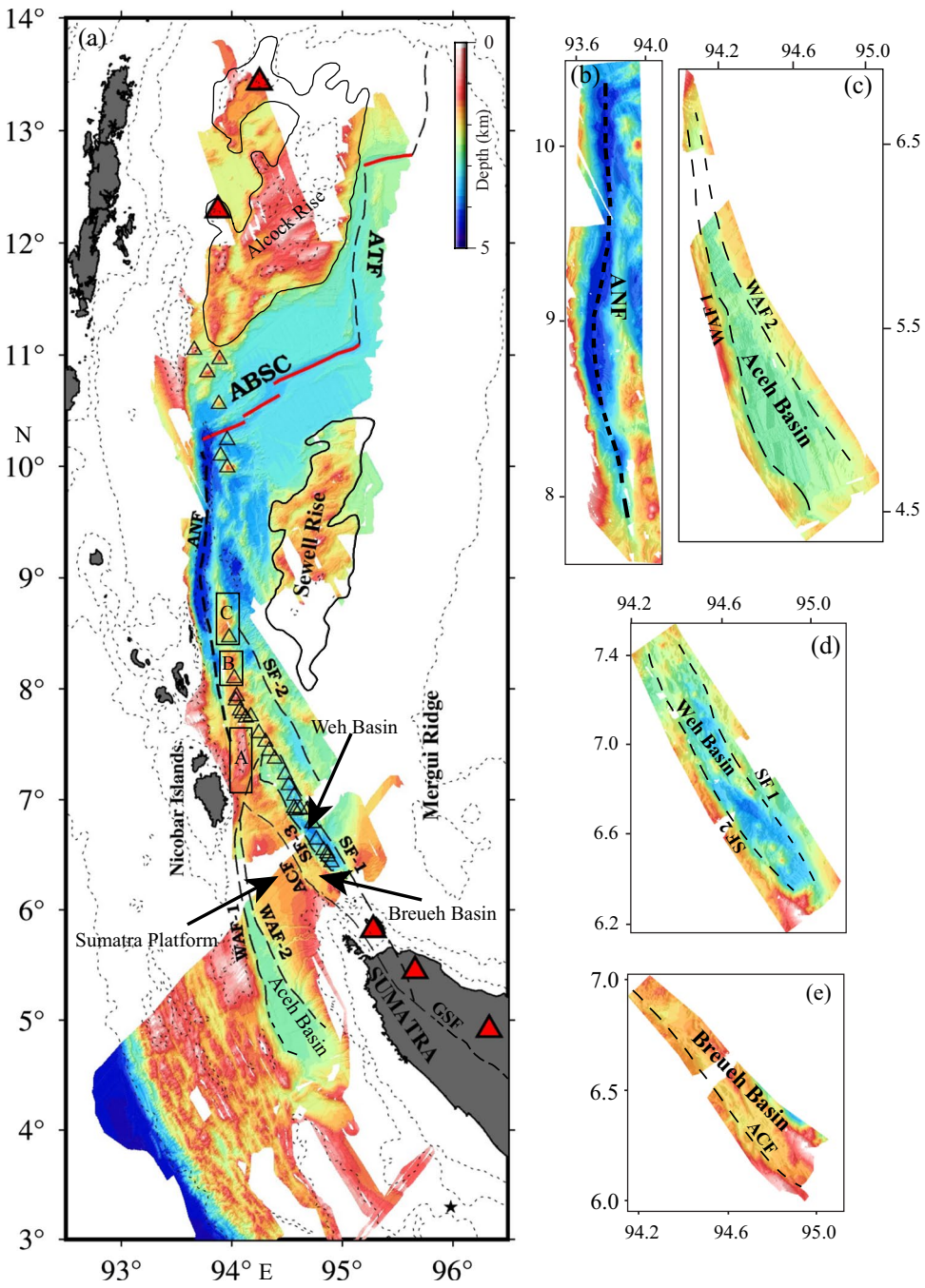

Fig. 2 **a** High-resolution multibeam bathymetry data of Andaman Backarc Basin and Sumatra region. The multibeam bathymetry data provided in Kamesh Raju et al. 2004, Graindorge et al. 2008, Yatheesh et al. 2021 are also compiled for this map. The dashed black lines represent the major faults, and the black outlined triangles indicate the submarine volcanoes identified from the bathymetry. The thick red lines indicate the Andaman Backarc Spreading Centre. ABSC: The black bordered red triangles represent the subaerial volcanoes (Sheth et al. 2009; Bandopadhyay and Carter 2017). ANF: Andaman-Nicobar Fault; WAF-1 and 2: two strands of West Andaman Fault; ACF: Aceh Fault; SF-1, 2 and 3: three strands of Seulimeum Fault. **b** Enlarged bathymetry image depicts the Andaman Nicobar Fault (ANF) located in the deep basin. **c** Enlarged bathymetry image of Aceh Basin. **d** Enlarged bathymetry image of Weh Basin. **e** Enlarged bathymetry image of Breueh Basin

of 600 m and display characteristics of deformation. Towards the northeastern part of this basin, a sedimented small push-up ridge (Figs. 3c & d) is present. Below the ridge feature, exists a thrust fault that dips to northeast, forming the boundary of the narrow basin. This basin, in turn, is bordered on its northeast side by a normal fault that dips to the southwest. The gravity profile shows low gravity up to -40 mGal along the deep scarp and narrow valley (Fig. 3b). Seen together with the bathymetry data, we can interpret that the southern tip of the ANF is lying in this narrow basin. Further northeast a volcanic cone and then a small valley bounded by thin sediment capped ridges are seen (Fig. 3c).

South of 7°N the WAF is bifurcated into two faults WAF-1 and WAF-2, and these strands make a deep graben like feature which is called as Aceh Basin. The Aceh Basin, which has a triangle shape and a length of around 270 km, is bounded to the east by the Sumatra platform and to the west by the fore-arc high of the inner accretionary wedge (Figs. 2a & c). This basin has a width of approximately 10 km in the northern region adjacent to

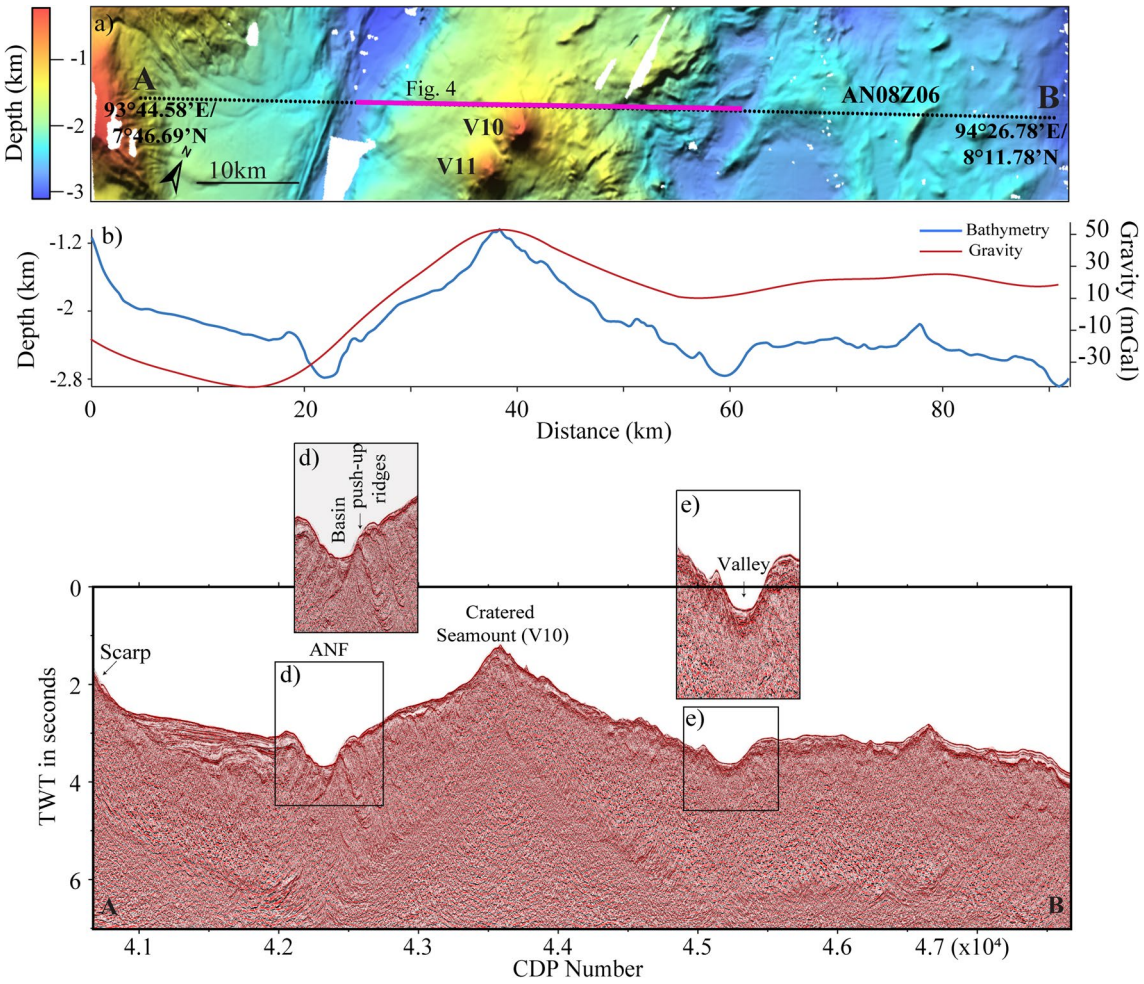

Fig. 3 **a** Location map of seismic section AN08Z06. Black dashed line is the seismic line location and pink line represent the location of zoomed seismic section shown in Fig. 4. **b** Gravity anomaly(red) and bathymetry (blue) over the seismic profile. **c** Seismic reflection image of AN08Z06. **d** Enlarged image of push-up ridge and basin in the west. **e** Enlarged seismic image of deep valley in the east

Nicobar Island. As one progresses southward, the width of the basin expands to about 50 km (Fig. 2c).

The GSF originates from the Sumatra mainland and splits into two branches in the offshore region: the western ACF and the eastern SF. Two strands of SF make a deep graben like feature, termed as Weh Basin, and it is approximately 80 km in its width and 115 km in length (Figs. 2a & d). The deeper region in the Weh Basin reaches up to 3600 m water depth and consists of submarine volcanoes. The rhombic shaped Weh Basin is considered to have formed by a releasing step fault related to SF (Ghosal et al. 2012). A rugged elevated topographic feature referred as 'push-up ridge' following the same trend of Weh Basin is located between Weh Basin and Aceh fault. Another narrow basin called Breueh Basin (Figs. 2a & e), that is shallow compared to the other basins, located east of the Aceh fault widens towards south.

Sumatra platform is ~ 60 km wide, extends from the southeast of Nicobar Island, located between WAF and ACF, have a gentle topography between 1000 and 2000 m water depth (Fig. 2a). This terminates around 7°N where the WAF and ACF converge. This platform is considered as the offshore continuation of the Sumatra continental block (Singh et al. 2012).

Submarine volcanic arc

The submarine volcanic arc is a major feature in the Andaman Sea that provides a link between the Barren Island and the volcanic system in Sumatra. The ~ 564 km stretch of this submarine volcanic arc between 6°24'N and 11°N has been examined in this study. Within this region, thirty-three different volcanoes of varying heights and sizes have been mapped (Figs. 5, 6, 7, Table 1 and Supplementary figures S1-S5). V1 is the northernmost volcano, with a conical

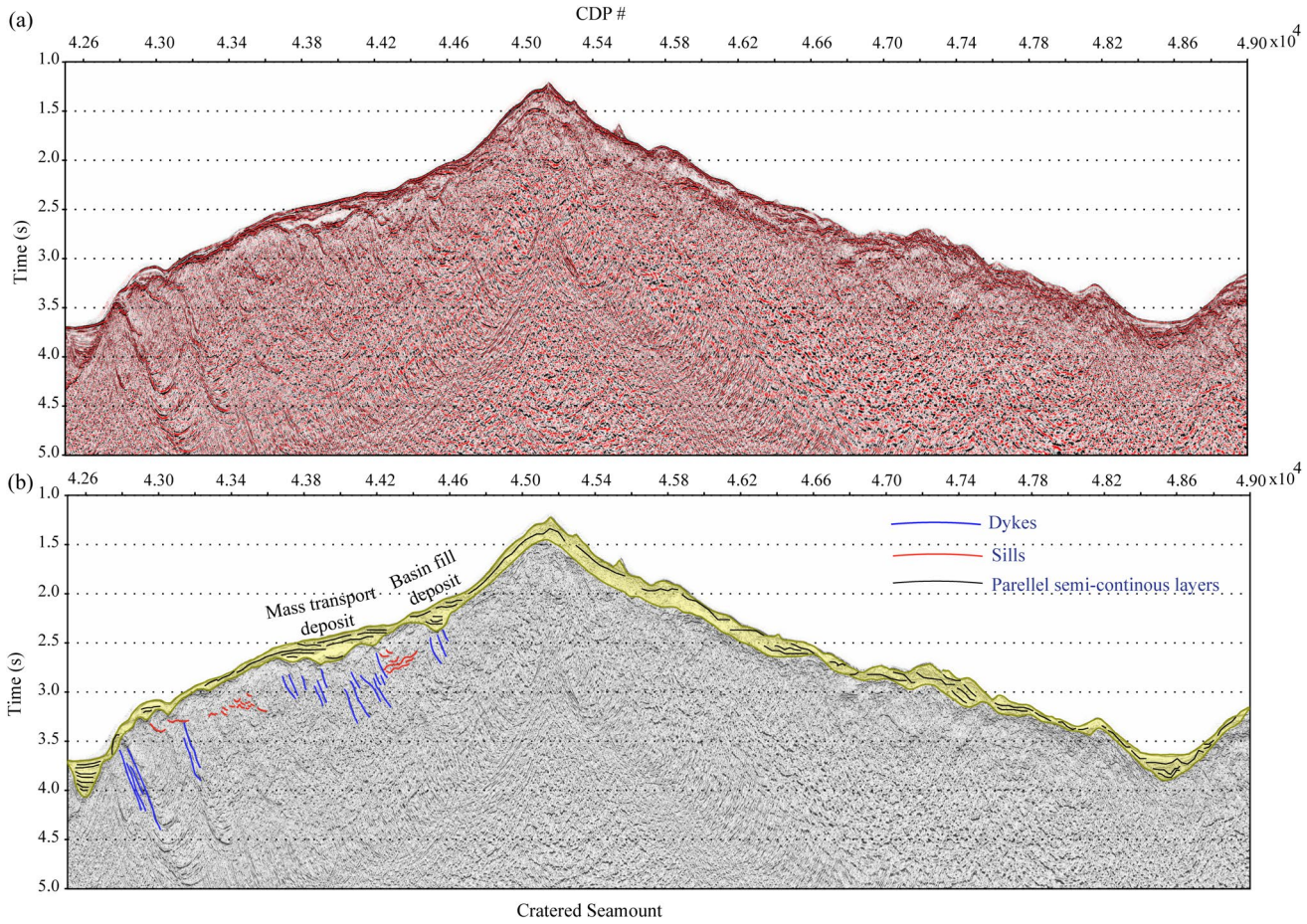

Fig. 4 **a** Seismic reflection section of AN08Z06 (Location shown as pink line in Fig. 3a), (**b**) Interpreted Seismic reflection section of AN08Z06

shape and a height of 2155 m (Figs. 5a & b, Table 1, Supplementary figure S1a). Volcano V2, located 26 km to the southeast of V1, has a collapsed top area (cratered) with a total height of 1435 m (Figs. 5a & b, Table 1, Supplementary figure S1b). Volcano V3 has an uneven shape and a SSW-NNE general trend (Figs. 5a & b, Table 1, Supplementary figure S1c). The conical-shaped volcano V4 is located on the flat ocean floor and has a height of 1485 m overall (Figs. 5a & b, Table 1, Supplementary figure S1d). A 2.3 km-diameter formation that resembles a caldera can be found over V4's northern flank. The volcanoes V1 to V4 are situated north of the spreading centre in the Andaman Backarc Basin (Figs. 5a & b). Volcano V5 is a conical-shaped volcano with a height of 1350 m that is situated across an irregular surface, south of the spreading centre (Figs. 5a & b, Table 1, Supplementary figure S2a). Volcano V6 has a roughly conical shape and is in a flat seabed basin (Figs. 5a & b, Table 1, Supplementary figure S2b). V7 is near to V6, which covers an area of 728 km^2 (Figs. 5a & b, Table 1, Supplementary figure S2c). V7 is the highest of the identified volcanoes, with a total height of 2455 m and an erratic shape with several summits. Volcanoes V1 to V7 line up with ANF (Fig. 5a). The V1-V4 are located on the northern part of the Segment A of the ABSC and V5, V6 and V7 are in the southern part of the spreading centre.

From the V7 towards the south, there is a conspicuous gap of 169 km in the occurrence of arc volcanoes between 8.4°N to 9.9°N. After this gap, 26 volcanoes are documented in the Off Nicobar region (Figs. 6 & 7, Table 1). This part of the volcanic arc chain has a deep graben shaped structure towards the east of WAF and west of step-like fault system of SF, and it is the northward extension of the Weh Basin. Volcano V8, is located off the Nicobar region at a water depth of 2350 m and rises to 680 m above the surrounding terrain (Figs. 6a & 6b, Table 1, Supplementary figure S3a). V8 exhibits a well-defined crater having a depth of 300 m and a maximum width of ~ 2.5 km (Figs. 6a & 6b, Table 1, Supplementary figure S3a). South of this V8, rugged elevated topographic feature about 15 km in length is present that resembles a push-up ridge like feature. Volcano V9 has a roughly conical shape and is located about 40 km south of volcano V8 and rises to a height of 740 m (Figs. 6a & 6b,

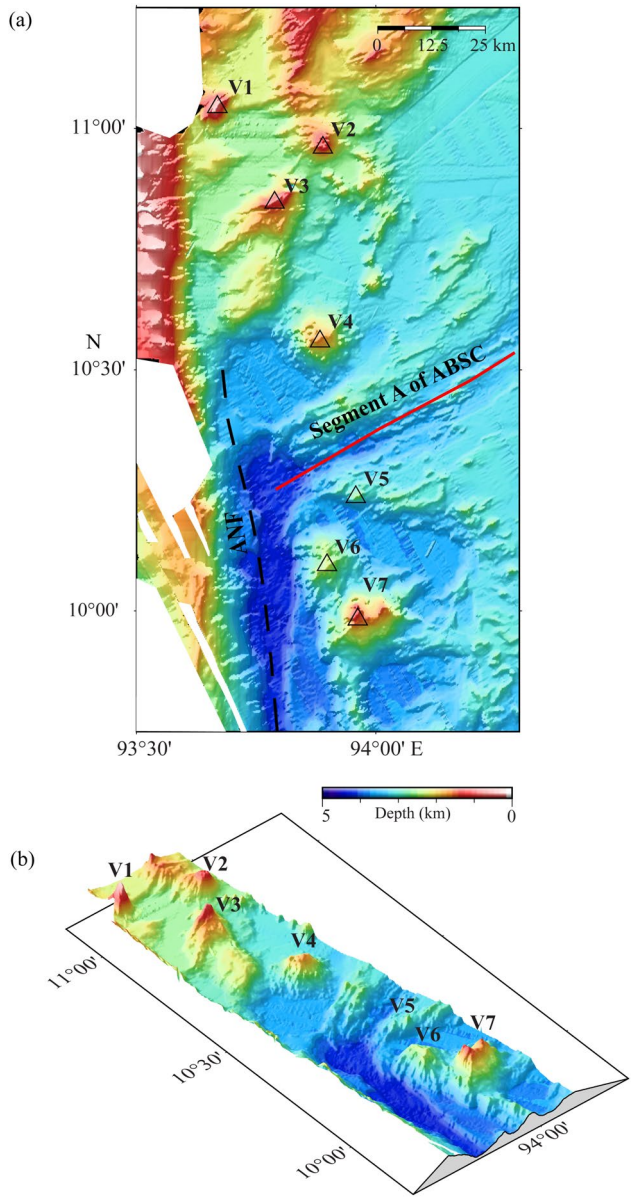

Fig. 5 **a** High Resolution multibeam bathymetry map of submarine volcanoes V1-V7. **b** 3D image of the volcanic arc in the north

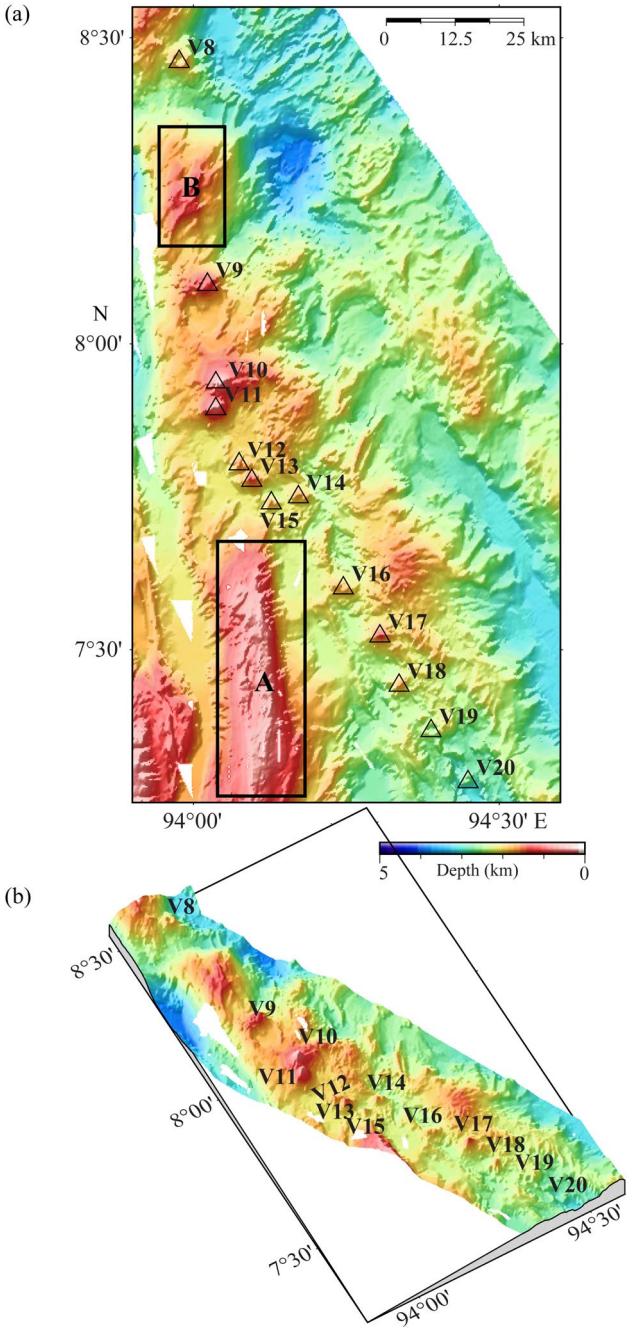

Fig. 6 **a** High Resolution multibeam bathymetry map of submarine volcanoes V8-V20. **b** 3D image of the volcanic arc in the off Nicobar region

Table 1, Supplementary figure S3b). Volcanoes V10 and V11, which are very close by were named cratered seamount (CS) (Kamesh Raju et al. 2012a). These volcanoes are of 1180 m and 1005 m height, respectively, and occupy an area of ~ 90 km^2 (Figs. 6a & 6b, Table 1, Supplementary figure S3c). The well-defined breach in the crater (approximately 800 m width and 100 m depth) and the seabed samples from the crater indicate that these volcanoes erupted in the recent geological past.

The seismic line nearest to the crater seamount is depicted in Fig. 4, passing approximately 15 km from the seamount's center. The seismic section near to cratered seamount (V10) shows an existence of wide conical feature spanning 20 km in width, with an elevation reaching up to 800 m in water depth. The sides of this cone display sediment layers up to 100 m in thickness, while the remainder of the cone lacks sediment deposits. The seismic data suggest (Fig. 4b) that the volcanic rocks are buried beneath 50–250 m thick sedimentary layers appearing as parallel semi-continuous layers that warp the volcanic rocks. Notably, a mass-transport

deposit, characterized by acoustically transparent layers, is evident between CDPs 43,600 and 44,100, while a small basin fill deposit is observed between CDPs 44,400 and 44,600 (Figs. 4a & 4b). The seismic data also reveal numerous near-vertical dyke intrusions within the volcanic rocks alongside some semi-horizontal intrusions or sills.

The volcanoes V12 to V15 are smaller in size and closely spaced to each other with a distance of ~ 4–5 km and exhibits similar morphology (Figs. 6a & 6b, Table 1). V12, V13, and V14 are all aligned in the same direction, while V15 is located on the eastern side of V14. These 4 volcanoes are situated on the rugged and elevated topography (Figs. 6a & 6b, Table 1, Supplementary figure S3d, S3e). South of V15, four volcanoes (V16-V19) are evenly distributed with a distance of ~ 10–11 km apart from each other. V16's summit is irregularly shaped; unlike other volcanoes, it lacks an overall conical shape. Its flanks likewise have an uneven morphology (Fig. 6a, Table 1, Supplementary figure S3f). The heights of V17 and V18 are 760 m and 820 m, respectively, and both exhibit morphology with a conical shape that is identical (Figs. 6a & 6b, Table 1, Supplementary figure S4a, S4b). V19, which is located at a sea depth of 2500 m and has a height of 210 m, has the shape of a collapsed crater (Figs. 6a & 6b, Table 1, Supplementary figure S4c). The maximum width of the crater is ~ 2.5 km.

Further south, we have identified fourteen distinct volcanoes (V20-V33) in the graben-like depression between 6°24' N and 7°24' N (Figs. 7a & 7b, Table 1). Compared to V8-V19 volcanoes which are situated in the elevated topography in the off Nicobar region, these southern 16 volcanoes are situated in the deeper basin. The volcanoes V20-V23 are conical in shape with steep flanks on either side, situated in the bathymetric depression i.e., the Weh Basin (Fig. 7a). Volcanoes V20-V23 are located at smooth seafloor around 3080 m to 3300 m water depth and possess height ranging from 375 m (V20) to 915 m (V23) with an averaging spacing of 12 km (Figs. 7a & 7b, Table 1, Supplementary figure S4d-g).

Closely spaced volcanoes V24, V25 and V26 are nearly conical in shape having rugged summit area with a total relief of 765 m, 600 m and 900 m respectively (Figs. 7a & 7b, Table 1, Supplementary figure S4h). V27 and V28 are associated with the escarpment of SF and exhibit similar morphology. These exhibit an elongated shape in the NNW-SSE direction with irregular flanks. These volcanoes are separated at a distance of 13 km and exhibit a height of 715 m and 1050 m respectively for V27 and V28 (Figs. 7a & 7b, Table 1, Supplementary figure S4h, S5a). V29 is located in the Weh Basin and has a height of 755 m (Figs. 7a & 7b, Table 1, Supplementary figure S5b). Volcanoes V30-V33 are located close to each other

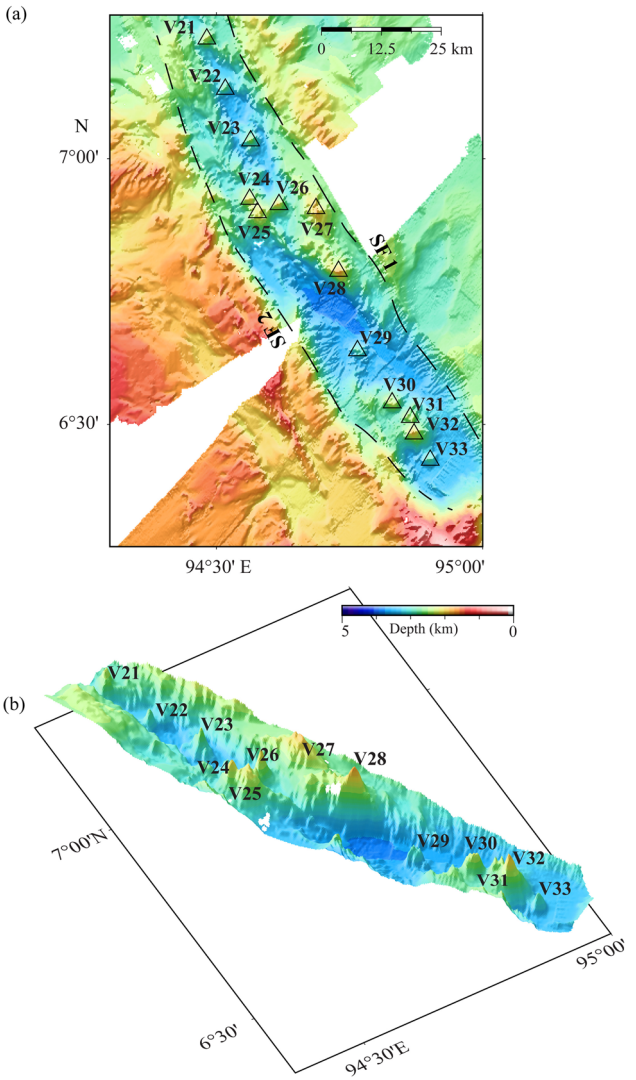

Fig. 7 **a** High Resolution multibeam bathymetry map of submarine volcanoes V21-V33. **b** 3D image of the volcanic arc in the south towards Sumatra Island

(~ 4–7 km apart) with conical shape situated in the smooth seafloor of Weh Basin (Figs. 7a & 7b, Table 1). V30 having a total height of 690 m exhibits a crater shape at the summit with a maximum width of 630 m which is less compared to the cratered seamounts in the northern region (Supplementary figure S5c). Volcanoes V31-V33 occupies an area of ~ 60 km^2 and possess height of 560 m, 855 m and 495 m respectively for V31, V32 and V33 (Figs. 7a & 7b, Table 1, Supplementary figure S5d).

A distinct large gap (169 km) of distance in active volcanoes V7 and V8 between 8.6°N and 9.8°N is quite prominent (Figs. 2 & 8). We have also observed distinct variations in the spacing between the volcanoes and their physical dimensions (Fig. 8). The distance from volcano V1 to V33

Table 1 Characteristics of volcanoes (V1-V33) in the Andaman Sea. Table 1 provides the location, height, basal length, basal width, basal area and height-width ratio of each volcano, and distance between adjacent volcanoes

Volcano	Centre Location (Degree)		Depth(m)		Height (m) H	Basal Length (km)	Basal-Width (km)	Basal Area (sq.km)	H-W ratio (2H/Wb)	Distance from the adjacent Volcano
			Summit	Basal						
V1	93.6689	11.04	355	2510	2155	11.5	10.3	118.45	0.418	0
V2	93.8894	10.9617	1080	2515	1435	11.2	14.2	159.04	0.202	26
V3	93.7884	10.8478	830	2605	1775	25	15.7	392.5	0.226	20.5
V4	93.8834	10.5604	1595	3080	1485	18.5	20	370	0.148	34
V5	93.958	10.2378	2410	3730	1320	6.5	5.2	33.8	0.507	38
V6	93.8979	10.0967	2230	3730	1500	16.6	19.3	320.38	0.155	17.5
V7	93.9622	9.98444	1225	3680	2455	28	26	728	0.188	17
V8	93.9765	8.46215	1695	2375	680	5.3	5	26.5	0.272	169
V9	94.0228	8.09817	1125	1865	740	6	5.3	31.8	0.279	40
V10	94.0441	7.93556	360	1540	1180	7.6	5.7	43.32	0.414	18
V11	94.0366	7.89491	595	1600	1005	6	5.5	33	0.365	4.5
V12	94.0747	7.80486	1490	1975	485	3.5	3	10.5	0.323	11.2
V13	94.0954	7.77796	1310	2075	765	5.8	4.9	28.42	0.312	3.8
V14	94.1717	7.75107	1730	2250	520	3.9	3.5	13.65	0.297	5.2
V15	94.1274	7.74106	1650	2030	380	3.5	2.9	10.15	0.262	5.1
V16	94.245	7.602	1710	2170	460	6.3	6.1	38.43	0.151	18.5
V17	94.3049	7.52343	1240	2000	760	5.7	5.6	31.92	0.271	11.4
V18	94.3361	7.44275	1635	2455	820	6.3	5.5	34.65	0.298	10.2
V19	94.3886	7.3685	2290	2500	210	4.8	4.3	20.64	0.098	10.3
V20	94.4488	7.28496	2705	3080	375	4.2	3.3	13.86	0.227	19.6
V21	94.482	7.22562	2280	3085	805	6	4.3	25.8	0.374	11.2
V22	94.5168	7.13128	2685	3165	480	4.8	3.5	16.8	0.274	12.7
V23	94.5644	7.03419	2390	3305	915	8.3	5.3	43.99	0.345	12.5
V24	94.5626	6.92428	2030	2795	765	3.8	4.9	18.62	0.312	3.2
V25	94.5773	6.90229	2135	2735	600	5.1	6.3	32.13	0.190	4.5
V26	94.6176	6.9142	1945	2880	935	4.4	4.6	20.24	0.407	8
V27	94.6872	6.90687	1825	2540	715	10.3	6	61.8	0.238	14.2
V28	94.7293	6.78872	1760	2820	1060	9.1	7.8	70.98	0.272	13.2
V29	94.765	6.63942	2865	3620	755	7.4	6	44.4	0.252	17.4
V30	94.8301	6.54142	2270	2960	690	5.3	6.3	33.39	0.219	13.2
V31	94.864	6.51394	2325	2885	560	4.1	4.2	17.22	0.267	5
V32	94.8713	6.4828	1900	2755	855	4.6	6.1	28.06	0.280	3.6
V33	94.9015	6.43334	2840	3335	495	4.1	3.8	15.58	0.261	6.7

versus height and area of the volcanoes clearly shows that the height and base area of the volcanoes V1-V7 are relatively high when compared to the V8-V33 volcanoes. The volcanoes (V8-V33) are closely spaced and smaller in physical dimension (area) when compared to volcanoes (V1-V7) present in the northern sector of the Andaman Sea (Fig. 8). The spacing between the volcanoes is 17 to 38 km for the northern volcanoes (V1-V7) and it is about 9 to 19 km for the southern off Nicobar volcanoes.

Discussion

The Neogene Inner Arc volcanic system in the Andaman-Nicobar-Sumatra subduction zone encompasses a volcanic arc extending from northern extinct volcanoes like Mt. Popa and Mt. Wuntho in Myanmar to southern active volcanoes in the Sumatra through subaerially exposed dormant Narcondam Island, active Barren Island and submarine volcanoes in the Andaman Sea (Haldar et al. 1992; Curray 2005), the total span is over 2000 km long.

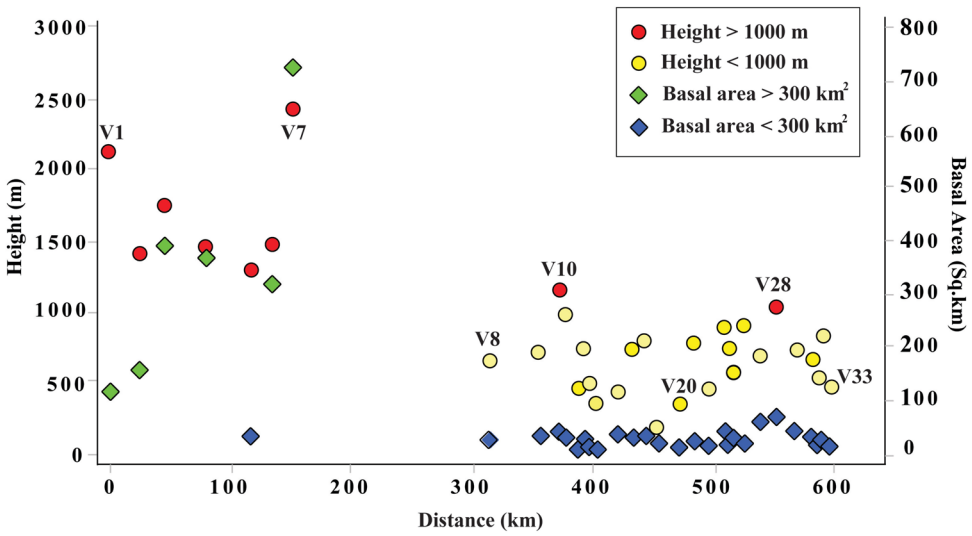

Fig. 8 The graph showing the distance of volcanoes measured with respective to V1, versus height (red circle indicates height > 1000 m and yellow circle indicates height < 1000 m) and area (green square indicates area > 300 km^2 and blue square indicates area < 300 km.^{2}) of each volcano (V1-V33) from north (93.6°E, 11.04°N) to south (94.9°E, 6.43°N)

Myanmar, located at the northern end of the volcanic arc, has a complicated tectonic setting where highly oblique subduction takes place. This region is characterised by the presence of the Burmese Microplate which separates the Indian plate from the Burma plate and is surrounded by important fault systems, including Churachandpur-Mao (CM) Fault to the west (e.g., Gahalaut et al. 2013) and Sagaing Fault to the east (Bertrand et al. 1998; Curray 2005; Maurin and Rangin 2009). This section of the subduction system is characterized by nearly trench parallel subduction and rate of convergence varies from 14 mm/yr to 34 mm/yr. From the geochemical analysis the quaternary volcanoes Wuntho, Monwya, and Popa (Wuntho-Monywa-Popa arc) present in the central Myanmar basin are thought to have developed by melting a previously metasomatized mantle wedge and these volcanoes are distinct for their short life and limited magmatic productivity (Lee et al. 2016). The distance between these volcanoes varies from 166 to 223 km. The volcanic activity in Myanmar is attributed to the region's deep geodynamics and its position above a slab tearing window due to the oblique subduction. This window, located beneath the Burmese plate at mantle depths, allows Indian oceanic lithosphere to detach from continental lithosphere, influencing Myanmar's volcanic activity's spatial distribution and characteristics (Lee et al. 2016).

Moving southward into the Andaman Sea region, the obliquity in the subducting plate decreases when compared to north Myanmar. The Sagaing Fault, believed to have originated in the middle to late Eocene, around 44 Ma, was initially identified as the sliver fault (Curray 2005; Singh et al. 2013). This fault system in Myanmar is intricately linked to the Andamana Nicobar Fault (ANF), West Andaman Fault (WAF) and Great Sumatra Fault (GSF) systems further south, forming a network of transform faults and connecting to the spreading center (Andaman Backarc Spreading Center) in the central Andaman Sea basin (Curray 1979; Curray 2005). Sieh and Natawidjaja (2000) proposed that the GSF, located on the mainland of Sumatra, started its activity around 2 Ma ago. It is suggested that the sliver fault in the Andaman Sea could have also shifted to become the ANF around the same time (Singh and Moeremans 2017). Through in-depth studies involving seismic reflection and refraction, Singh et al. (2012) proposed that the WAF is likely a back thrust, but later studies suggested that WAF is considered as strike-slip fault (Martin et al. 2014; Ghosal et al. 2021).

In the Andaman Sea, the recent volcanic activity has been recorded on Barren Island, which has frequent eruptions, while Narcondam is inactive. The Andaman Backarc Spreading centre and Andaman Nicobar Fault shapes the geological topography of the Andaman Sea, allowing for relative motion between the Indian plate and the Burma microplate. The inner arc volcanic chain of the Andaman Islands, situated between the east of Andaman and Nicobar Island and the west of Sewell and Alcock rises, exhibits distinctive geomorphological features. This volcanic arc chain comprises two sub-aerial volcanic islands, Barren Island and Narcondam Island, along with thirty-three prominent submarine seamounts and numerous smaller seamounts of varying heights and diameters. Geodetic measurements suggest that southwest convergence at Barren Island and northeast motion at Narcondam, indicating the diverse tectonic processes at work in the area. Out of 33 distinct volcanoes, 5 volcanoes are characterized as cratered volcanoes (V2, V8, V10, V19 and V30). The cratered volcanoes having rugged topography and seems to comprise of hard substratum depict their eruptive history in the recent past. In particular, the region off Nicobar is dominated by several cratered

seamounts and fissure fracture features, which were most likely created by volcanic activity in the recent geological past. In the seismic profile (Fig. 4), numerous near-vertical dyke intrusions within the volcanic rocks, alongside some semi-horizontal intrusions or sills, resemble observations in the Romney volcanic field offshore New Zealand (Bischoff et al. 2021). Earthquake studies also indicate significant activity in the off Nicobar region, notably the occurrence of very long period hybrid earthquake swarms, attributed to magma movement (Aswini et al. 2020, 2021). These observations suggest the region between 6ºN to 8ºN is the most active part of the volcanic arc during the recent past. Recent study by Sriram et al. 2023 observed for the first time two gas flares originating from the outer flanks of cratered seamount (V10) in the water column imaging data during the expeditions of 2018 and 2021. It is probable that the observed gas flares are induced by the perturbations in the subsurface shallow magma chamber. Detailed analysis of the gas emanations is required to ascertain their origin.

There is distinct gap in between the volcanoes V7 and V8 when compared to all the submarine volcanoes in the inner volcanic arc region. Earlier studies suggested that the subduction of base of the Ninetyeast Ridge was one of the possible reasons for the gap in volcanic activity in this region. Thick, buoyant roots underlying the Ninetyeast Ridge basement highs tend to flatten the subducting plate, inhibiting the subduction process and resulting in gaps in volcanism and seismicity, and deformation of the forearc (Subrahmanyam et al. 2008; Singha et al. 2019). Here, the detailed multibeam bathymetry helped us to confirm the gap in the volcanoes in support of the inferences of earlier studies.

Further south, along the islands of Sumatra and Java, the direction of subduction changes from approximately 60° near Sumatra to 90°off Java, indicating a reduction in the obliquity and an increase in the rate of convergence of subduction off Java (Cattin et al. 2009). The GSF fault system stretches along the western border of Sumatra and is connected with intense seismic activity and volcanic activity. A chain of volcanoes lines the western edge of Sumatra. The focal points of these volcanoes form a curvilinear pattern, unexpectedly shifting back and forth, altering the trajectory of the primary GSF (Sieh and Natawidjaja 2000). In Sumatra the quaternary volcanoes are unevenly dispersed, with the majority located north of the main volcanic arc. Some of these volcanoes are associated with structural components, such as the Seulimeum fault (Pacey et al. 2013). Java's volcanic arc, located within the larger tectonic framework of the Sunda Arc, saw significant volcanic activity during the Tertiary and Quaternary periods. Although not directly related to a major fault system, Java's volcanic landscape is influenced by regional tectonic pressures and interactions with other geological structures (Soeria-Atmadja and Noeradi 2005).

Volcanoes in normal subduction zones, such as the Izu-Bonin-Mariana volcanic arc or Aleutian arc in the Philippine Sea (Usui and Nishimura 1992; Ishizuka et al. 2006), the Tonga-Karmadec-Lau arc in the southwest Pacific (Ewart et al. 1998), and the Java-Sumatra arc system, are about 60 to 120 km apart. The volcanoes in oblique subduction zones, such as the Kuril Island arc in the NW Pacific (DeMets 1992; Glasby et al. 2006), the Lesser-Antilles volcanic arc (Calais et al. 2002), and the Andaman-Sumatra arc (Kamesh Raju et al. 2012a and current study), are more closely spaced, ranging from 3 to 30 km apart. This finding implies that oblique subduction and back arc rifting in the Andaman Sea most likely resulted in the creation of a zone in the westernmost part of the Andaman backarc region where the submarine volcanoes are very closely spaced. Volcanoes in the northern sector of the Andaman Sea are spaced differently probably due to local characteristics such as distance from the trench, age of the subducting plate from south to north, existence of active spreading centres, and magma supply. These variables could potentially explain the variations in volcano spacing. The size and spacing of the submarine volcano can be controlled by distribution of magma generated by subduction processes and related tectonic activities (England et al. 2004). The large submarine province identified in the Mariana Arc resembles a closely spaced characteristic (overall volcanic center density is 4.4/100 km of arc) while in the case of the Tonga-Kermadec arc bear volcanic density of 2.9/100 km (Baker et al. 2008). Spacing and distribution of the Andaman arc volcanoes shows different characteristics from some of the mapped submarine volcanoes which are unevenly distributed with varying physical dimension from small to large, similar to south New Hebrides volcanic arc (Patriat et al. 2015), south Aegean Active Volcanic Arc (Foutrakis and Anastasakis 2018) volcanism observed in this area. The dip angle of the subducting Indian plate increases progressively from the Nicobar segment (NS) to the Andaman segment (AS), with values of approximately 26°, 47°, and 53° respectively (Singha et al. 2019). This trend is supported by tomographic inversion data beneath the Andaman and Nicobar Islands (Kennett and Cummins 2005). Age plays a significant role in governing this variation, with the younger Indian plate in the Nicobar segment (60–80 million years old) exhibiting a lower dip angle due to greater buoyancy, compared to the older plate in the Andaman segment (~90–100 million years old) which subducts at a higher angle (Müller et al. 2008). Previous studies have indicated that the deformation modes in overriding plates of convergent margins are significantly influenced by both the dip angle and age of the subducting slab. Shallow dip angles ($<30°$) and young ages (<60 Ma) tend to promote compressional deformation, while steeper dip angles ($>50°$) and older ages (>60 Ma) favor extensional deformation (Dasgupta et al. 2021). These relationships dictate the tectonic styles observed at convergent margins, where compressional stresses typically result in

prominent forearc wedges and narrow backarc basins, whereas tensile stresses lead to wide extensional backarc basins and minor forearc wedges. In the context of the Andaman Sea region, the presence of backarc spreading indicates extensional deformation. Furthermore, the higher dip angle observed in the Andaman Segment compared to the Nicobar Segment could contribute to the formation of a backarc basin in the northern part of the region. This suggests that the variation in dip angles along the subduction zone plays a significant role in shaping the tectonic features and deformation styles observed in the Andaman Sea area. According to McCaffrey (2009), the convergence rate off the coast of Sumatra is estimated to be approximately 40 to 50 mm/yr. However, this rate decreases to less than 20 mm/yr off the Andaman-Nicobar subduction zone. This variation in convergence rates is primarily attributed to oblique convergence, where the relative motion between the two converging plates is not purely perpendicular to the subduction trench. Given that the subduction rate is higher in the Nicobar region compared to the Andaman region, this could potentially lead to increased dehydration and release of fluids from the subducting slab. The presence of abundant magma can lead to the formation of a larger number of volcanoes in the Nicobar region compared to the Andaman region. The availability of more magma increases the volcanic activity in the region. Therefore, the higher subduction rate in the Nicobar region may play a role in the geological activity and volcanic hazards observed in this area. In contrast to the continental part of the overriding plate found in northern Myanmar and southern Sumatra, the Andaman-Nicobar segment is characterized by an ocean-ocean collision setting. This distinction is significant and may contribute to the abundance of volcanoes observed in the vicinity of the Nicobar region.

Conclusion

This study presents an examination of the morphotectonic features of the Andaman Backarc region, with a special emphasis on the inner volcanic arc, sliver fault system, and small oceanic basins in the Andaman backarc region. The discovery of 33 submarine volcanoes and fault networks in the Andaman Sea was made possible by the high-resolution multibeam bathymetry data.

When compared to other volcanic arcs throughout the world, volcanoes in the Andaman-Sumatra arc region, vary in size and distribution, influenced by factors such as subduction direction, distance from the trench, age of the subducting plate, and magma supply. This results in distinct patterns of volcanic activity, with closely spaced submarine volcanoes in off Nicobar region and uneven distribution towards the north. Also, the presence of an ocean-ocean collision setting in the Andaman-Nicobar segment contributes to the abundance of volcanoes observed in the vicinity of the Nicobar region, distinguishing it from adjacent regions with continental overriding plates. The existence of well-developed crater morphology, frequent occurrence of earthquake swarms and gas emanations through the flanks of the crater seamounts suggest intense active volcanism in the off Nicobar region.

The Andaman backarc region is characterised by several narrow basins and graben structures that are impacted by sliver fault systems such as ANF, WAF and GSF. The presence of fault networks and basins reflect the Andaman Sea's complicated tectonic processes and stress distribution.

Supplementary Information The online version contains supplementary material available at https://doi.org/10.1007/s00367-024-00775-4.

Acknowledgements We extend our sincere gratitude to Prof. Sunil Kumar Singh, the Director of CSIR-National Institute of Oceanography (NIO), for his unwavering support and encouragement throughout this research. KAKR and CMB thank Dr. Thamban Meloth, Director, NCPOR for the support and encouragement. We are thankful to the shipboard scientific parties of the expeditions SSK-33, SSK-49, and SSD-046 for their help and support in acquisition of the data. We thank Directorate General of Hydrocarbons (DGH), Ministry of Petroleum & Natural Gas for providing the seismic data and allow us for the use of the data for research purpose. Special thanks go to Dr. Graindorge and Prof. Satish Singh from IPGP, Paris, for generously providing the published bathymetry grid data in the NW Sumatra region. We thank the anonymous reviewers for their constructive comments and suggestions which helped us to improve the manuscript. This work was carried out under TeaM-RiSe and OLP2004 projects of CSIR-National Institute of Oceanography. This work is a CSIR-NIO contribution 7262.

Author contribution Conceptualization, Writing Original Draft: KKA, KAKR.

Supervision, Resources, Project administration : KAKR, VY, PD

Data quality check, Data processing, Plotting figures: KKA, CMB, NFKZ

Review & Editing: KKA, KAKR, CMB, VY, NFKZ, PD

Funding Council of Scientific and Industrial Research (CSIR) provided the financial support for research carried out under the TeaM-RiSe and OLP2004 projects at the CSIR-National Institute of Oceanography.

Data Availability All the data presented in this paper are avilable at CSIR-National Institute of Oceanography, Goa.

Declarations

Competing interests The authors declare no competing interests.

Code availability Not applicable.

Ethics approval Not Applicable.

Consent to participate Not Applicable.

Consent for publication Certified that all authors have seen and approved the final version of the manuscript being submitted.

References

Acocella V, Bellier O, Sandri L, Sébrier M, Pramumijoyo S (2018) Weak tectono-magmatic relationships along an obliquely convergent plate boundary: Sumatra. Indonesia Front Earth Sci 6:3

Aswini KK, Dewangan P, Kamesh Raju KA, Yatheesh V, Singha P, Arya L, Ramakrushana Reddy T (2020) Sub-surface magma movement inferred from low-frequency seismic events in the off-Nicobar region. Andaman Sea Sci Rep 10:21219

Aswini KK, Kamesh Raju KA, Dewangan P, Yatheesh V, Singha P, Reddy R (2021) Seismotectonic evaluation of off Nicobar earthquake swarms. Andaman Sea J Asian Earth Sci 221:104948. https://doi.org/10.1016/j.jseaes.2021.104948

Aswini KK, Kamesh Raju KA, Dewangan P, Yatheesh V, Singha P, Reddy R (2022) Insights into the long period earthquakes detected by ocean bottom seismometer experiment in the Andaman Sea. IEEE Express, Oceans-2022. pp 1–7. https://doi.org/10.1109/OCEANSChennai45887.2022.9775319

Baker ET, Embley RW, Walker SL, Resing JA, Lupton JE, Nakamura KI, de Ronde CEJ, Massoth GJ (2008) Hydrothermal activity and volcano distribution along the Mariana arc. J Geophys Res 113:B08S09. https://doi.org/10.1029/2007JB005423

Bandopadhyay PC, Carter A (2017) Chapter 2 Introduction to the geography and geomorphology of the Andaman–Nicobar Islands. Geol Soc Lond Mem 47(1):9–18

Belousov A, Belousova M, Zaw K, Streck MJ, Bindeman I, Meffre S, Vasconcelos P (2018) Holocene eruptions of Mt. Popa, Myanmar: Volcanological evidence of the ongoing subduction of Indian Plate along Arakan Trench. J Volcanol Geotherm Res 360:126–138

Bertrand G, Rangin C, Maury RC, Htun HM, Bellon H, Guillaud JP (1998) The Singu basalts (Myanmar): New constraints for the amount of recent offset on the Sagaing Fault. Comptes Rendus De L'academie Des Sciences Series IIA Earth Planet Sci 7(327):479–484

Bertrand G, Rangin C (2003) Tectonics of the western margin of the Shan plateau (central Myanmar): implication for the India-Indochina oblique convergence since the Oligocene. J Asian Earth Sci 21(10):1139–1157

Bischoff A, Planke S, Holford S, Nicol A (2021) Seismic Geomorphology, Architecture and Stratigraphy of Volcanoes Buried in Sedimentary Basins. Updates in Volcanology - Transdisciplinary Nature of Volcano Science. IntechOpen., Available at: https://doi.org/10.5772/intechopen.95282.

Calais E, Mazabraud Y, Mercier de Lépinay B, Mann P, Mattioli G, Jansma P (2002) Strain partitioning and fault slip rates in the northeastern Caribbean from GPS measurements. Geophys Res Lett 29:3-1–3-4

Cattin R, Chamot-Rooke N, Pubellier M, Rabaute A, Delescluse M, Vigny C, Fleitout L, Dubernet P (2009) Stress change and effective friction coefficient along the Sumatra-Andaman-Sagaing fault system after the 26 December 2004 (Mw= 9.2) and the 28 March 2005 (Mw= 8.7) earthquakes. Geochem Geophys Geosyst 10(3) https://doi.org/10.1029/2008GC002167

Chhibber HL (1934) Geology of Burma. McMillan, London, p 538

Cochran JR (2010) Morphology and tectonics of the Andaman Forearc, northeastern Indian Ocean. Geophys J Int 182:631–651

Curray JR (2005) Tectonics and history of the Andaman Sea region. J Asian Earth Sci 25:187–232

Curray JR, Moore DG, Lawver LA, Emmel FJ, Raitt RW, Henry M, Kieckhefer R (1979) Tectonics of the Andaman Sea and Burma: convergent margins. Am Assoc Pet Geol Mem 29:189–198

Dasgupta R, Mandal N, Lee C (2021) Controls of subducting slab dip and age on the extensional versus compressional deformation in the overriding plate. Tectonophysics 801:228716. https://doi.org/10.1016/j.tecto.2020.228716

DeMets C (1992) Oblique convergence and deformation along the Kuril and Japan Trenches. J Geophys Res Solid Earth 97:17615–17625

Diehl T, Waldhauser F, Cochran JR, Kamesh Raju KA, Seeber L, Schaff D, Engdahl ER (2013) Back-arc extension in the Andaman Sea: Tectonic and magmatic processes imaged by high-precision teleseismic double-difference earthquake relocation. J Geophys Res Solid Earth 118:2206–2224

England P, Engdahl R, Thatcher W (2004) Systematic variation in the depths of slabs beneath arc volcanoes. Geophys J Int 156(2):377–408

Ewart A, Collerson KD, Regelous M, Wendt JI, Niu Y (1998) Geochemical Evolution within the Tonga–Kermadec–Lau Arc–Back-arc Systems: the Role of Varying Mantle Wedge Composition in Space and Time. J Petrol 39:331–368

Fitch TJ (1972) Plate convergence, transcurrent faults, and initial deformation adjacent to southeast Asia and the western Pacific. Geophys Res 77:4432–4460

Foutrakis PM, Anastasakis G (2018) The active submarine NW termination of the South Aegean Active Volcanic Arc: The Submarine Pausanias Volcanic Field. J Volcanol Geotherm Res 357:399–417. https://doi.org/10.1016/j.jvolgeores.2018.05.008

Gahalaut VK, Kundu B, Laishram SS, Catherine J, Kumar A, Singh MD, Tiwari RP, Chadha RK, Samanta SK, Ambikapathy A, Mahesh P (2013) Aseismic plate boundary in the Indo-Burmese wedge, northwest Sunda Arc. Geology 41:235–238. https://doi.org/10.1130/g33771.1

Ghosal D, Mukti MM, Singh SC, Carton H, Deighton I (2021) Forearc high and basin evolution offshore northern Sumatra using high-resolution marine geophysical datasets. J Asian Earth Sci 216:104814

Ghosal D, Singh SC, Chauhan APS, Hananto ND (2012) New insights on the offshore extension of the Great Sumatran fault, NW Sumatra, from marine geophysical studies. Geochem Geophys Geosyst 13. https://doi.org/10.1029/2012GC004122

Glasby GP, Cherkashov GA, Gavrilenko GM, Rashidov VA, Slovtsov IB (2006) Submarine hydrothermal activity and mineralization on the Kurile and western Aleutian island arcs, N.W. Pacific Mar Geol 231:163–180

Graindorge D, Klingelhoefer F, Sibuet JC, McNeill L, Henstock TJ, Dean S, Gutscher MA, Dessa JX, Permana H, Singh SC, Leau H, White N, Carton H, Malod JA, Rangin C, Aryawan KG, Chaubey AK, Chauhan A, Galih DR, Greenroyd CJ, Laesanpura A, Prihantono J, Royle G, Shankar U (2008) Impact of lower plate structure on upper plate deformation at the NW Sumatran convergent margin from seafloor morphology. Earth Planet Sci Lett 275:201–210

Halder D, Laskar T, Bandopadhyay PC, Sarkar NK, Biswas JK (1992) Volcanic eruption of the Barren island volcano, Andaman Sea. J Geol Soc India 39:411–419

Hariyono E, Liliasari S (2018) The characteristics of volcanic eruption in Indonesia. Volcanoes: Geological and Geophysical Setting, Theoretical Aspects and Numerical Modeling, Applications to Industry and Their Impact on the Human Health. p 73. https://doi.org/10.5772/intechopen.71449

Htet TTZ, Nishimura T, Hashimoto M, Lindsey EO, Aung LT, Min SM, Thant M (2022) Present-day crustal deformation and slip rate along the southern Sagaing fault in Myanmar by GNSS observation. J Asian Earth Sci 228:105125

Ishizuka O, Kimura JI, Li YB, Stern RJ, Reagan MK, Taylor RN, Ohara Y, Bloomer SH, Ishii T, Hargrove US, Haraguchi S (2006) Early stages in the evolution of Izu-Bonin arc volcanism: New age, chemical, and isotopic constraints. Earth Planet Sci Lett 250:385–401

Kamesh Raju KA, Ramprasad T, Rao PS, Ramalingeswara Rao B, Varghese J (2004) New insights into the tectonic evolution of the Andaman basin, northeast Indian Ocean. Earth Planet Sci Lett 221:145–162

Kamesh Raju KA, Murty GPS, Amarnath D, Kumar MLM (2007) The west Andaman fault and its influence on the aftershock pattern of the recent megathrust earthquakes in the Andaman-Sumatra region. Geophys Res Lett 34:1–5

Kamesh Raju KA, Ray D, Mudholkar A, Murty GPS, Gahalaut VK, Samudrala K, Paropkari AL, Ramachandran R, Prakash LS (2012a) Tectonic and volcanic implications of a cratered seamount off Nicobar Island. Andaman Sea J Asian Earth Sci 56:42–53

Kamesh Raju KA, Mudholkar A, Murty GPS, Yatheesh V, Singh SC, Kiranmai S, Moeremans R (2012b) Multibeam mapping of the West Andaman Fault, NW Sumatra Fault, Andaman volcanic arc and their tectonic and magmatic implications. Abstract T41C-2608 presented at 2012 Fall Meeting. AGU, San Francisco, Calif., pp 3–7. https://ui.adsabs.harvard.edu/abs/2012AGUFM.T41C2608K

Kamesh Raju KA, Aswini KK, Yatheesh V (2020) Tectonics of the Andaman Backarc Basin – Present Understanding and Some Outstanding Questions, IGC-2020 Commemorative Volume, The Andaman Islands and Adjoining Offshore: Geology. Society of Earth Scientists, Springer, Tectonics and Paleoclimate

Kennett BL, Cummins PR (2005) The relationship of the seismic source and subduction zone structure for the 2004 December 26 Sumatra-Andaman earthquake. Earth Planet Sci Lett 239(1–2):1–8

Lee H-Y, Chung S-L, Yang H-M (2016) Late Cenozoic volcanism in central Myanmar: Geochemical characteristics and geodynamic significance. Lithos 245:174–190. https://doi.org/10.1016/j.lithos.2015.09.018

Martin KM, Gulick SP, Austin JA Jr, Berglar K, Franke D, Udrekh, (2014) The West Andaman Fault: A complex strain-partitioning boundary at the seaward edge of the Aceh Basin, offshore Sumatra. Tectonics 33(5):786–806

Maurin T, Rangin C (2009) Structure and kinematics of the Indo-BurmeseWedge: Recent and fast growth of the outer wedge. Tectonics 28:TC010. https://doi.org/10.1029/2008tc002276

McCaffrey R (2009) The tectonic framework of the Sumatra subduction zone. Annual Rev Earth Planet Sci 37:345–366

Moeremans RE, Singh SC (2015) Fore-arc basin deformation in the Andaman-Nicobar segment of the Sumatra-Andaman subduction zone: Insight from high-resolution seismic reflection data. Tectonics 34:1736–1750

Müller RD, Sdrolias M, Gaina C, Roest WR (2008) Age, spreading rates, and spreading asymmetry of the world's ocean crust. Geochem Geophys Geosyst 9:Q04006. https://doi.org/10.1029/2007GC001743

Pacey A, Macpherson CG, McCaffrey KJW (2013) Linear volcanic segments in the central Sunda Arc, Indonesia, identified using Hough Transform analysis: Implications for arc lithosphere control upon volcano distribution. Earth Planet Sci Lett, Volumes 369–370:24–33. https://doi.org/10.1016/j.epsl.2013.02.040

Patriat M, Collot J, Danyushevsky L, Fabre M, Meffre S, Falloon T, Rouillard P, Pelletier B, Roach M, Fournier M (2015) Propagation of back-arc extension into the arc lithosphere in the southern New Hebrides volcanic arc. Geochem Geophys Geosyst 16:3142–3159. https://doi.org/10.1002/2015GC005717

Rangin C, Maw W, Lwin S, Naing W, Mouret C, Bertrand G, and GIAC scientific party (1999) Cenozoic pull apart basins in central Burma; the trace of the path of India along the western margin of Sundaland. Paper presented at European Union of Geosciences conferences, Strasbourg, France.

Rock NM, Syah HH, Davis AE, Hutchison D, Styles MT, Lena R (1992) Permian to recent volcanism in northern Sumatra, Indonesia: a preliminary study of its distribution, chemistry, and peculiarities. Bull Volcanol 45:127–152

Rodolfo KS (1969) Bathymetry and marine geology of Andaman Basin, and tectonic implications for southeast Asia. Geol Soc Amer Bull 80(7):1203–1230. https://doi.org/10.1130/0016-7606(1969)80[1203:BAMGOT]2.0.CO;2

Sandwell DT, Harper H, Smith TB, WH, (2021) Gravity field recovery from geodetic altimeter missions. Adv Space Res 68(2):1059–1072

Sheth HC, Ray JS, Bhutani R, Smitha KA, RS, (2009) Volcanology and eruptive styles of Barren Island: an active mafic stratovolcano in the Andaman Sea, NE Indian Ocean. Bull Volcanol 71:1021–1039

Sieh K, Natawidjaja D (2000) Neotectonics of the Sumatran fault, Indonesia. J Geophys Res Solid Earth 105:28295–28326

Singh SC, Moeremans R (2017) Chapter 13 Anatomy of the Andaman Nicobar subduction system from seismic reflection data. Geol Soc Lond Mem 47:193–204

Singh SC, Chauhan AP, Calvert AJ, Hananto ND, Ghosal D, Carton RA, H, (2012) Seismic evidence of bending and unbending of subducting oceanic crust and the presence of mantle megathrust in the 2004 Great Sumatra earthquake rupture zone. Earth Planet Sci Lett 321:166–176

Singh SC, Moeremans R, McArdle J, Johansen K (2013) Seismic images of the sliver strike-slip fault and back thrust in the Andaman-Nicobar region. J Geophys Res Solid Earth 118:5208–5224

Singha P, Dewangan P, Kamesh Raju KA, Aswini KK, Ramakrushana Reddy T (2019) Geometry of the Subducting Indian Plate and Local Seismicity in the Andaman Region from the Passive OBS Experiment Geometry of the Subducting Indian Plate and Local Seismicity in the Andaman Region. Bull Seismol Soc Am 109:797–811

Soeria-Atmadja R, Noeradi D (2005) Distribution of Early Tertiary volcanic rocks in south Sumatra and west Java. Island Arc 14:679–686. https://doi.org/10.1111/j.1440-1738.2005.00476.x

Sriram G, Dewangan P, Yatheesh V, Peketi A, Mahesh P, Mazumdar A, Mahale VP, Jacob J, Dubey KM, Mishra KP, CK, et al (2023) Gas migration signatures over the volcanic cratered seamount, off the Nicobar Islands in the Andaman Sea. Geo-Mar Lett 43(3):16

Subrahmanyam C, Gireesh R, Chand S, Kamesh Raju KA, Rao DG (2008) Geophysical characteristics of the Ninetyeast Ridge-Andaman island arc/trench convergent zone. Earth Planet Sci Lett 266:29–45

Taylor B, Crook K, Sinton J (1994) Extensional transform zones and oblique spreading centers. J Geophys Res 99(B10):19707–19718. https://doi.org/10.1029/94JB01662

Thompson G, Melson WG (1972) Petrology of oceanic crust across fracture zones in Atlantic Ocean—Evidence of a new kind of seafloor spreading. J Geol 80(5):526–538. https://doi.org/10.1086/627779

Tripathi SK, Nagendran G, Karthikeyan M, Vasu P, Tripathy SK, Varghese S, Raghav S, Resmi S (2017) Morphology of submarine volcanic seamounts from inner volcanic arc of Andaman Sea. Indian J Geosci 71:451–470

Tsutsumi H, Sato T (2009) Tectonic geomorphology of the southernmost Sagaing fault and surface rupture associated with the May 1930 Pegu (Bago) earthquake. Myanmar Bull Seismol Soc Am 99(4):2155–2168

Usui A, Nishimura A (1992) Submersible observations of hydrothermal manganese deposits on the Kaikata Seamount, Izu-Ogasawara (Bonin) Arc. Mar Geol 106(3–4):203–216

Uyeda S, Kanamori H (1979) Back-arc opening and the mode of subduction. J Geophys Res 84(Nb3):1049–1061. https://doi.org/10.1029/JB084iB03p01049

Yatheesh V, Aswini KK, Kamesh Raju KA, John Savio J, Dewangan P (2021) Morphotectonic signatures and revised timing of opening of the Andaman Basin. Northeast Indian Ocean Tectonophysics 820:229108. https://doi.org/10.1016/j.tecto.2021.229108

Zaw K, Swe W, Barber AJ, Crow MJ, New YY (2017) Introduction to the geology of Myanmar. Geol Soc Lond Mem 48:1–17